Studies on evaluation of bilirubin glucuronidation activity in canine and human primary hepatocytes cultured in a 3D culture system

March 2024

HISAYOSHI OMORI

CONTENTS

CONTENTS 2
1. INTRODUCTION 5
2. COMPARATIVE ANALYSIS OF BILIRUBIN GLUCURONIDATION ACTIVITY IN CANINE AND HUMAN PRIMARY HEPATOCYTES USING A 3D CULTURE SYSTEM 9
2.1. Introduction 9
2.2. Materials and methods 11
2.3. Results 14
2.4. Discussion 18
3. EVALUATING VARIATIONS IN BILIRUBIN GLUCURONIDATION ACTIVITY BY PROTEASE INHIBITORS IN CANINE AND HUMAN PRIMARY HEPATOCYTES CULTURED IN A 3D CULTURE SYSTEM 21
3.1. Introduction 21
3.2. Materials and methods 23
3.3. Results 28
3.4. Discussion 33
4. OVERALL DISCUSSION 37
5. OVERALL SUMMARY 40
6. ACKNOWLEGEMENT 42
7. REFERENCES 43

LIST OF FIGURES

Figure 1: Bilirubin production and metabolite. 5

Figure 2: Inhibition of bilirubin uptake into hepatocyte, glucuronidation and excretion by protease inhibitors. 7

Figure 3: Inhibition of bilirubin uptake into hepatocyte, glucuronidation and excretion by protease inhibitors. 8

Figure 4: Spheroid development images of (a) canine and (b) human primary hepatocytes on day 7, and (c) canine and (d) human primary hepatocytes on day 14 using the 3D culture system. Scale bar: 100 µm. 15

Figure 5: Representative liquid chromatography–mass spectrometry (LCMS) chromatograms of culture supernatants from (a) canine and (b) human primary hepatocytes 24 hours after bilirubin co-incubation in the 3D culture system for bilirubin, bilirubin mono-glucuronide, and di-glucuronide. 16

Figure 6: (a) Bilirubin mono-glucuronide formation and (b) bilirubin di-glucuronide formation 24 hours after co-incubation of bilirubin with canine and human primary hepatocytes cultured for 7 and 14 days in a 3D culture system. The generation of bilirubin glucuronides was expressed as the relative amount divided by the index of viability. *$P < 0.05$ compared with dogs. Data are expressed as mean ± S.D. All experiments were repeated six times. 17

Figure 7: Schematic representation from cell seeding to a test compound and bilirubin treatment, supernatant sampling, and cytotoxicity assessment in the 3D culture. 25

Figure 8: Albumin secretion from (a) canine and (b) human primary hepatocytes. Each plot indicates the mean ± standard deviation (S.D.) (n = 4). Spheroid development images of (c) canine and (d) human primary hepatocytes on Day 8 in the 3D culture system. Scale bar; 100 µm. (e) Relative expression of *UGT1A1* in canine and human primary hepatocytes on Day 8 in the 3D culture system. Each graph indicates the mean ± S.D. (n = 4). ***: p< 0.001 compared with canines. 30

Figure 9: Viabilities of canine and human primary hepatocytes exposed to atazanavir, indinavir, ritonavir, and nelfinavir for 48 hours. Each graph indicates the mean value (n = 5). 31

Figure 10: Evaluating the inhibition of bilirubin mono- and di-glucuronide generations after treatment with atazanavir, indinavir, ritonavir, and nelfinavir in (a) canine and (b) human primary hepatocytes cultured in the 3D culture system. Each graph indicates the mean ± S.D. (n = 4–5). *: p< 0.025 **: p< 0.005 ***: p< 0.0005 compared with the 0 µM group. 32

LIST OF TABLES

Supplementaly Table 1: Canine and human common probe and primer sequences for quantitative real-time polymerase chain reaction 24

1. INTRODUCTION

Bilirubin is the toxic end product of heme degradation when phagocytic cells, primarily macrophages, remove aged red blood cells. Finally, the produced bilirubin is released into the circulating blood, and unconjugated bilirubin bound to albumin is circulated tthroughout the body, reaching the liver, where it is removed from the plasma. Subsequently, within the cytoplasm of hepatocytes, bilirubin is bound to ligandin and transported to the endoplasmic reticulum, conjugating with glucuronic acid (Sticova and Jirsa 2013). Conjugation is primarily catalyzed by a conjugating enzyme, UDP-glucuronosyltransferase (UGT) 1A1 (Kadakol, et al. 2000). Glucuronidation is essential for eliminating bilirubin. Finally, conjugated bilirubin is eliminated from the body (Figure 1, Chen and Tukey 2018).

Figure 1: Bilirubin production and metabolite.

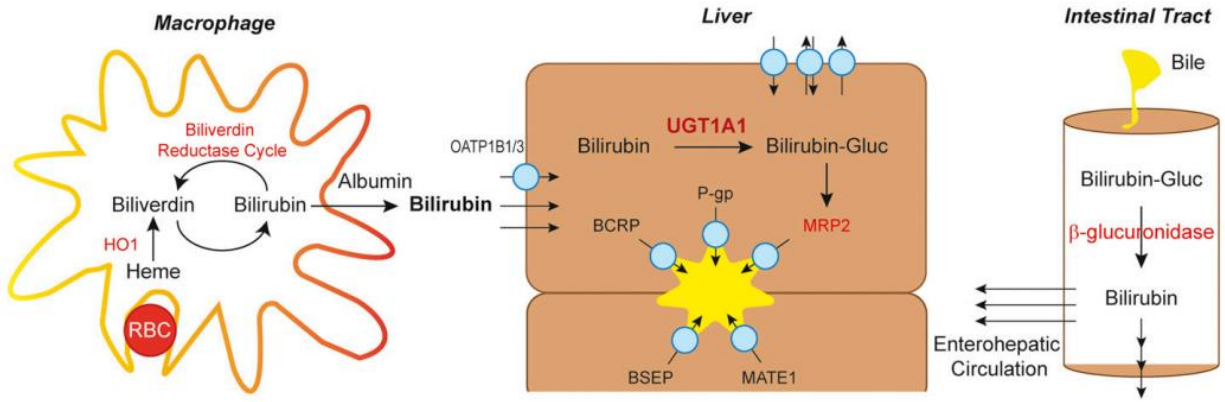

Several genetic polymorphisms of UGT1A1 have been reported in humans and have shown varying degrees of defective bilirubin conjugation. This results in decreased bilirubin clearance (Erlinger, et al. 2014). In addition, species differences in bilirubin glucuronidation activity have been identified between humans and dogs by liver microsomes and recombinant UGT1A1; dogs have lower activity than humans (Soars, et al. 2001; Troberg, et al. 2015). Non-clinical toxicity studies of new pharmaceutical compounds use rodents, usually rats, and non-rodents such as

dogs. However, as in the case of bilirubin, species differences in metabolism appear to influence the interpretation of non-clinical toxicity information. Therefore, it is critical to understand the differences in metabolic characteristics between humans and animals to extrapolate the results of non-clinical experiments to humans. An appropriate and detailed evaluation of pharmaceutical compounds, including species differences, adequately describes their toxicological information.

The liver is the major organ where the biotransformation of pharmaceutical compounds and other substances occurs, and *in vitro* models of drug biotransformation should resemble *in vivo* models. As popular *in vitro* models, hepatocytes or liver microsomes are commonly used to study drug metabolism (Brandon, et al. 2003). Hepatocytes are the most realistic system for complementing drug metabolic enzymes in a more physiological cellular environment. This system has shown a high success rate in predicting primary metabolites and metabolic pathways (Dalvie, et al. 2009). Regarding bilirubin glucuronidation activity, *in vitro* evaluations of bilirubin elimination using microsomes or recombinant UGT1A1 has been demonstrated (Ma, et al. 2014; Wang, et al. 2015); however, little information is available concerning the *in vitro* evaluation of bilirubin glucuronidation activity in hepatocytes. Although primary hepatocytes are useful and frequently used for the biotransformation of drugs, the drug metabolic activities of hepatocytes cultured in conventional two-dimensional (2D) conditions may differ from that of *in vivo* conditions due to changes in phenotypes, including the expression of drug-metabolizing enzymes or morphology. Therefore, the long-term stability of functioning hepatocytes is required in drug metabolism and pharmacokinetic studies (Hewitt, et al. 2007; Ohkura, et al. 2014).

In a three-dimensional (3D) culture system, hepatocytes form 3D aggregates called spheroids. Spheroid cultures support the maintenance of mature hepatic phenotypes, resulting in long-term stable hepatic functionality (Figure 2, Lauschke, et al. 2019). 3D hepatocyte culture

systems using primary hepatocytes are promising *in vitro* systems for studying drug metabolism (Bell, et al. 2016; Ohkura, et al. 2014).

Figure 2: Inhibition of bilirubin uptake into hepatocyte, glucuronidation and excretion by protease inhibitors.

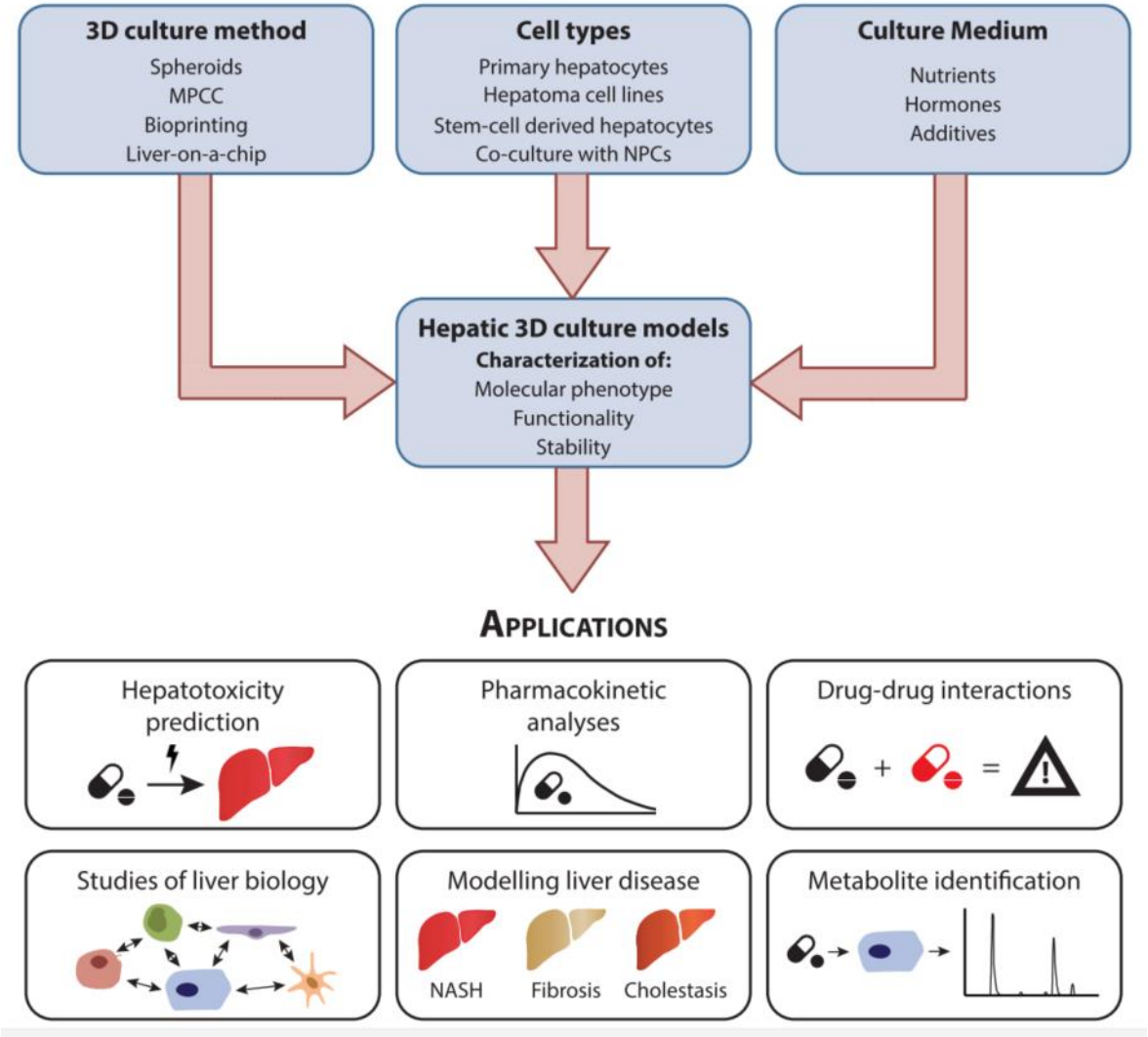

Drugs that inhibit hepatocyte uptake transporters (OATP1B1 and OATP1B3), glucuronidation enzyme for bilirubin (UGT1A1), and excretion transporter into bile (MRP2) may decrease bilirubin clearance and induce hyperbilirubinemia. Hyperbilirubinemia due to these effects is recognized as an adverse effect (toxicity) of drugs. Certain protease inhibitors are

known to cause clinical hyperbilirubinemia via inhibition of these enzymes and/or transporters (Figure 3, Chang, et al. 2013).

Figure 3: Inhibition of bilirubin uptake into hepatocyte, glucuronidation and excretion by protease inhibitors.

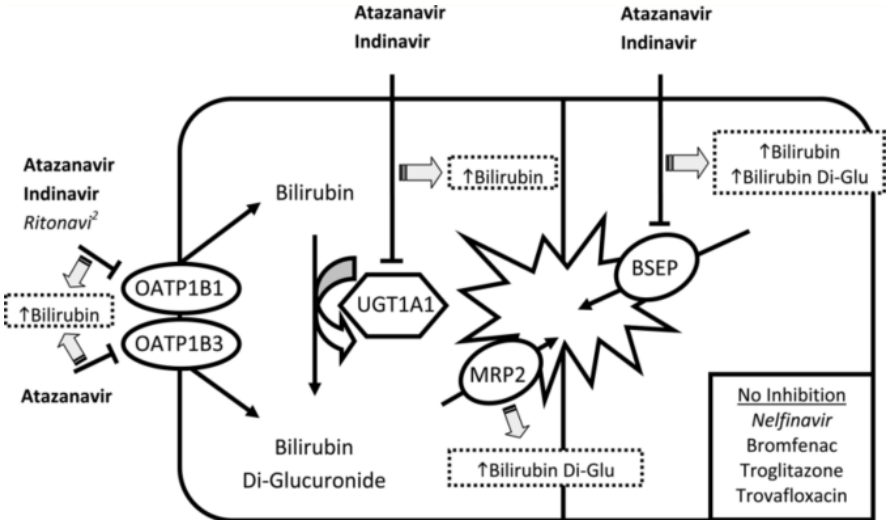

In this study, we conducted a comparative analysis of bilirubin glucuronidation activity in canine and human primary hepatocytes using a 3D culture system to verify the usefulness of 3D culture and primary hepatocyte and species differences for evaluating bilirubin metabolic function (Heading 1: Omori et al., 2022). Next, we evaluated the variations in bilirubin glucuronidation activity induced by protease inhibitors in canine and human primary hepatocytes cultured in a 3D culture system to confirm their utility in assessing the risk of bilirubin metabolic disorders for drug development (Heading 3: Omori et al., 2023) .

2. COMPARATIVE ANALYSIS OF BILIRUBIN GLUCURONIDATION ACTIVITY IN CANINE AND HUMAN PRIMARY HEPATOCYTES USING A 3D CULTURE SYSTEM

2.1. Introduction

Bilirubin is a byproduct of heme catabolism. When present in the bloodstream, unconjugated bilirubin binds to albumin and is transported to the liver, where it is extracted from plasma. Inside hepatocyte cytoplasm, bilirubin associates with ligandin and is then conveyed to the endoplasmic reticulum for conjugation with glucuronic acid (Sticova and Jirsa 2013). The conjugation process is primarily facilitated by UDP-glucuronosyltransferase (UGT) 1A1 (Kadakol et al. 2000). The resulting conjugated bilirubin is excreted into bile and eliminated from the body. Genetic polymorphisms in UGT1A1 can lead to impaired bilirubin conjugation, affecting bilirubin clearance (Aono et al. 1995; Bosma et al. 1995; Erlinger et al. 2014). The deficiency in bilirubin conjugation due to UGT1A1 inhibition results in various clinical implications and serves as a valuable tool for *in vitro*assessment of drug metabolism.

In vitro models employing hepatocytes or liver microsomes have been widely utilized to study drug metabolism (Brandon et al. 2003). Hepatocytes, possessing a full complement of drug-metabolizing enzymes, have proven to be more effective in generating biologically relevant metabolite profiles compared to liver microsomes (Dalvie et al. 2009). Despite the common use of human liver cell lines such as HepG2, drug metabolism activities of hepatocytes cultured in conventional two-dimensional (2D) conditions differ from those *in vivo* due to phenotypic changes, such as the expression of drug-metabolizing enzymes or morphology (Hewitt et al. 2007; Ohkura et al. 2014). This disparity is particularly noticeable in liver cell lines with lower expression levels of most drug-metabolizing enzymes than in primary hepatocytes (Brandon et al. 2003). To address these limitations, three-dimensional (3D) culture systems emerged in recent

years. Spheroids formed by hepatocyte aggregation in 3D culture systems replicate a more natural physiological environment, enabling the maintenance of mature hepatic phenotypes and stable hepatic functionality over the long term (Lauschke et al. 2019). The effectiveness of 3D culture systems has been demonstrated in studies involving liver cell lines like HepG2, HepaRG, and primary hepatocytes (Ohkura et al. 2014, Ramaiahgari et al. 2014, Takahashi et al. 2015, Bell et al. 2016). A previous study showed that evaluating bilirubin glucuronidation activity in HepG2 cells cultured in 2D conditions versus a 3D culture system was benefical for understanding bilirubin metabolic properties (Hirano et al. 2020).

In the development of new pharmaceuticals, safety studies in small- and medium-sized animals like mice and dogs are necessary. However, toxicity test results may vary among animal species, emphasizing the importance of analyzing factors contributing to species differences for human extrapolation. Thus far, differences in bilirubin glucuronidation activity have been observed between humans and dogs using liver microsomes and recombinant UGT1A1, with dogs exhibiting lower activity than humans (Soars et al. 2001; Troberg et al. 2015). While bilirubin elimination using microsomes or recombinant UGT1A1 has been reported (Ma et al. 2014; Wang et al. 2015), limited information is available regarding the *in vitro* assessment of bilirubin glucuronidation activity in liver cell lines or primary hepatocytes.

In the present study, bilirubin glucuronidation activity in canine and human primary hepatocytes was evaluated using a 3D culture system, and species differences in the activity between humans and dogs were compared.

2.2. Materials and methods

2.2.1. Cell culture

Bilirubin, acetonitrile, telmisartan, ammonium acetate, and dimethyl sulfoxide (DMSO) were purchased from FUJIFILM Wako Pure Chemical Corporation (Osaka, Japan). Culture media were purchased from Thermo Fisher Scientific (Waltham, MA, USA) unless otherwise stated. Cryopreserved primary hepatocytes from beagle dogs (male, five months old) and humans (five donors, 22–74 years old) were obtained from Thermo Fisher Scientific. The presence of mycoplasma below the detection level in both hepatocytes after thawing was confirmed by the Central Institute for Experimental Animals (Kanagawa, Japan) on February 16, 2022.

Canine and human primary hepatocytes were cultured for 7 and 14 days, respectively, according to the method of Ikeda et al. (2012), which is a microfabricated cell array system with minor modifications. Briefly, canine and human primary hepatocytes were prepared in William's medium E supplemented with a hepatocyte plating supplement pack (CM3000) and cryopreserved hepatocyte recovery medium (CM7000) after thawing, respectively. Cells were seeded at a density of 5.0×10^4 cells/well in 96-well 3D culture plates (Cell-able BP-96-R800, Toyo Gosei Co. Ltd., Tokyo, Japan), and cultured in William's medium E supplemented with CM3000 at 37 °C and 5% CO_2. The seeding medium was replaced with William's medium E supplemented with a hepatocyte maintenance supplement pack (CM4000) one day after seeding. The maintenance medium was replaced with half the amount of fresh medium every two or three days.

2.2.2. Cell treatment

Canine and human primary hepatocytes cultured in the 3D culture system were used for bilirubin glucuronidation assessment at 7 and 14 days after seeding. For bilirubin

glucuronidation assessment, the working solution was prepared by dissolving bilirubin in DMSO (20 mM), followed by addition of maintenance medium. Subsequently, the working solution was transferred to the wells and incubated at a concentration of the assessment (10 μM) in a humidified incubator at 37 °C and 5% CO_2. At 24 hours after incubation, the culture supernatant was collected and mixed with an equal amount of ice-cold 100% acetonitrile to terminate the reaction. Subsequently, the samples were centrifuged at 11,100 × *g* for 15 min at 4 °C, and the supernatants were stored at -80 °C until analysis. Although it is considered necessary to measure metabolites from both the cell pellet and its culture medium to assess the glucuronidation activity of bilirubin, for simplified application to an *in vitro* evaluation system, only the culture medium was measured to evaluate bilirubin metabolites excreted from hepatocytes.

2.2.3. Cell viability assay

The viability of cultured canine and human primary hepatocytes was examined using the Cell Titer-Glo® 3D cell viability assay kit (Promega, WI, USA) 24 hours after incubation with bilirubin on days 7 and 14. Briefly, a volume of Cell Titer-Glo® 3D reagent equal to the volume of the cell culture medium in each well was added to the culture wells. The contents of the wells were vigorously mixed for 30 minutes to induce cell lysis. This mixture was diluted 2-fold and the luminescent signal was measured using a Cytation 5 cell imaging multimode reader (BioTek Instruments, VT, USA) as an indicator of cell viability.

2.2.4. Liquid chromatography–mass spectrometry (LCMS) analysis

The internal standard (IS) stock solution was prepared by dissolving telmisartan in DMSO to a final concentration of 100 μg/mL. Working IS solution (100 ng/mL) was prepared by diluting the stock solution with acetonitrile. A total of 20 μL of the sample, 10 μL of IS working solution, and 60 μL of 10 mM ammonium acetate/acetonitrile (50:50, v/v) were mixed and

centrifuged at 2,000 × *g* for 2 min at 5 °C. After centrifugation, aliquots (10 μL) of the culture supernatants were injected into the LCMS system. The quantification of bilirubin, bilirubin mono-glucuronide, and bilirubin di-glucuronide was performed using high-performance liquid chromatography (HPLC; Shimadzu Prominence UFLC, Shimadzu Corporation, Kyoto, Japan) coupled with an electrospray ionization mass spectrometer (AB SCIEX Triple Quad 4500). HPLC separation was performed using an Accucore C18 column (2.6 μm, 2.1 × 50 mm, Thermo Fisher Scientific). The mass spectrometer was operated in the positive ion mode. MS data were collected through single ion monitoring as $[M+H]^+$ ions at 585 m/z for bilirubin, 761 m/z for bilirubin mono-glucuronide, 937 m/z for bilirubin di-glucuronide, and 515 m/z for telmisartan. The LCMS system was operated using Analyst 1.6.3 software (AB Sciex Pte. Ltd., Tokyo, Japan), and the data were processed using software. The relative amounts of bilirubin mono-glucuronide and di-glucuronide in canine and human primary hepatocytes were expressed as the target area divided by the IS area in the LCMS system. The generation of bilirubin glucuronides was expressed as the relative amount divided by the luminescence value of the Cell Titer-Glo® 3D cell viability assay, which was an index of viability that was calculated according to the following method:

$$\text{Generation of bilirubin glucuronides} = \frac{\text{Relative amounts of bilirubin glucuronides}^{w}}{\text{Luminescence value of 3D cell viability assay}}$$

In this equation, *w* is the value of the target area (Figure 5) that was divided by the IS area for each bilirubin glucuronide in the LCMS system.

2.2.5. Statistical analysis

The generation of bilirubin glucuronides in dogs and humans was evaluated using independent Student's t-test. Statistical significance was set at $P < 0.05$.

2.3. Results

When spheroid development in canine and human primary hepatocytes was evaluated using the cell array system for 3D cell culture on days 7 and 14 after the start of culture, canine hepatocyte spheroids had a more distinct spherical shape than human hepatocyte spheroids irrespective of the culture period (Figure 4).

When the glucuronidation activity of bilirubin was assessed in canine and human primary hepatocytes after 24 hours of incubation, the generation of mono- and di-glucuronides was detected in both canine and human primary hepatocytes (Figure 5).

After incubation with bilirubin for 24 hours on days 7 and 14, the mean luminescence values were higher in canine primary hepatocytes (1,319,479 and 1,414,890, respectively) than that in human primary hepatocytes (384,726 and 229,169, respectively). The generation of bilirubin mono- and di-glucuronides was significantly higher ($P < 0.05$) in human primary hepatocytes than those in canine primary hepatocytes, irrespective of the culture period (Figure 6).

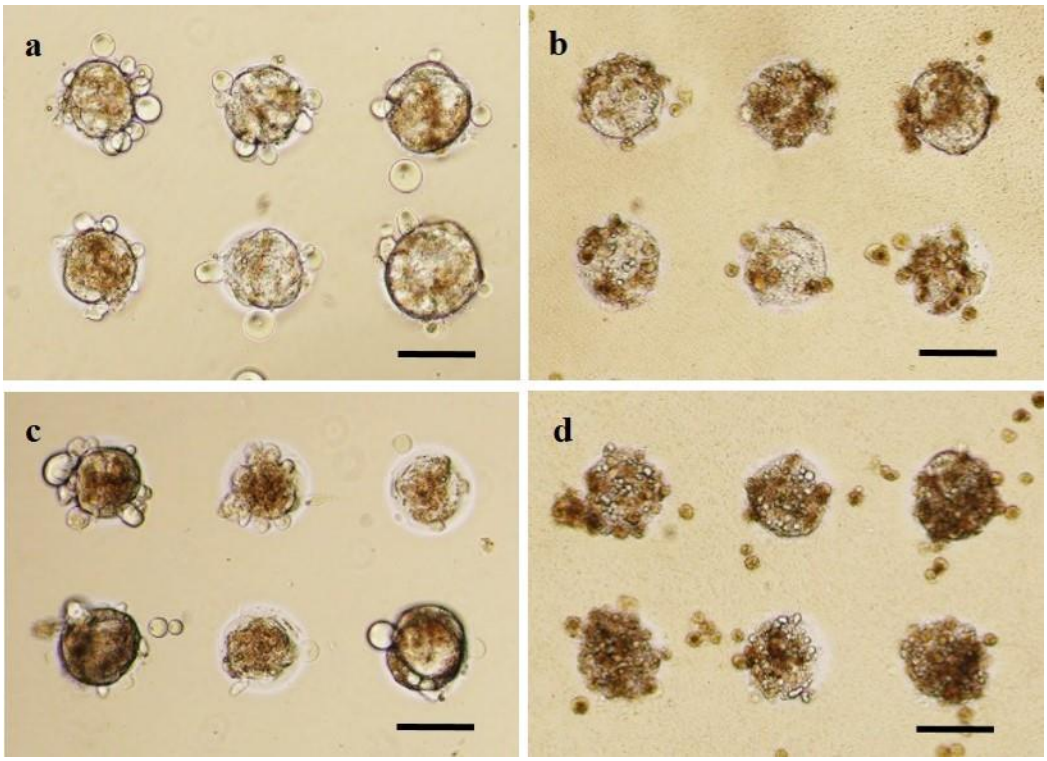

Figure 4: **Spheroid development images of (a) canine and (b) human primary hepatocytes on day 7, and (c) canine and (d) human primary hepatocytes on day 14 using the 3D culture system. Scale bar: 100 µm.**

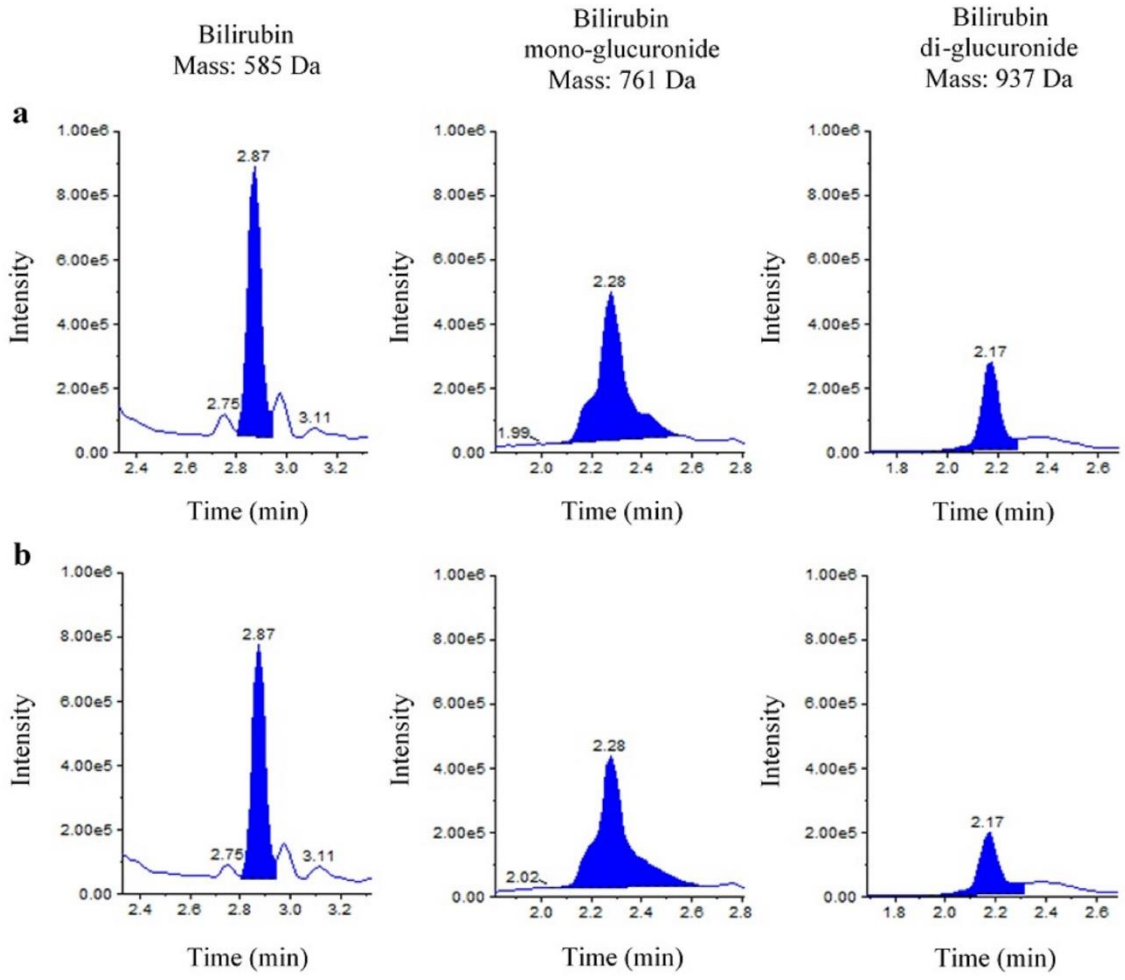

Figure 5: **Representative liquid chromatography–mass spectrometry (LCMS) chromatograms of culture supernatants from (a) canine and (b) human primary hepatocytes 24 hours after bilirubin co-incubation in the 3D culture system for bilirubin, bilirubin mono-glucuronide, and di-glucuronide.**

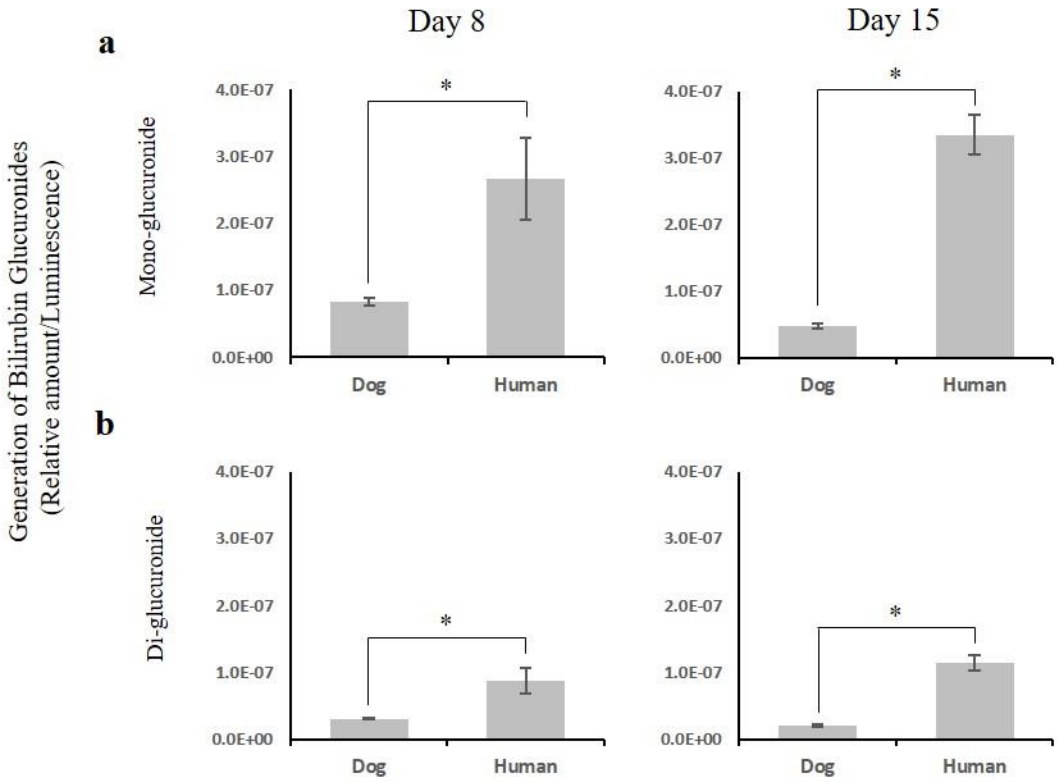

Figure 6: **(a) Bilirubin mono-glucuronide formation and (b) bilirubin di-glucuronide formation 24 hours after co-incubation of bilirubin with canine and human primary hepatocytes cultured for 7 and 14 days in a 3D culture system. The generation of bilirubin glucuronides was expressed as the relative amount divided by the index of viability. *$P < 0.05$ compared with dogs. Data are expressed as mean ± S.D. All experiments were repeated six times.**

2.4. Discussion

To date, there have been documented instances of hepatocyte culture in human using a 3D culture system (Ogihara et al. 2017, Ohkura et al. 2014), but there is a dearth of information regarding the *in vitro* evaluation of bilirubin glucuronidation activity in canine hepatocytes cultured within a 3D culture system. In this investigation, we observed that canine primary hepatocytes cultured for 7 and 14 days on cell culture plates developed spherical structures. A comparative analysis of canine and human hepatocyte spheroids on days 7 and 14 revealed a more pronounced spherical shape in the canine spheroids. However, the spheroid morphology in both species remained consistent until day 14, aligning with prior reports (Ogihara et al. 2017). Notably, human hepatocyte spheroids exhibited an increase in single cells that were not integrated with the spheroid on day 14, indicating the presence of dead cells. Consequently, spheroid status was evaluated based on cell proliferation and apoptosis. In a previous study, we reported that utilizing the 3D culture system with Cell-able plate for the human hepatoma cell line HepG2 proved more effective in assessing bilirubin metabolic characteristics than in a 2D culture system (Hirano et al. 2020). Other studies have also demonstrated that 3D-cultured hepatoma cell lines exhibit higher expression of metabolic enzymes, such as UGT1A1 and transporters, as well as increased metabolic activities for exogenous compounds (Kobayashi et al. 2012, Ramaiahgari et al. 2014). Hepatoma cell lines generally exhibit lower metabolic enzyme activities than primary hepatocytes, including UGT1A1, responsible for bilirubin glucuronidation (Guo et al. 2011, Westerink and Schoonen 2007, Wilkening et al. 2003). This study detected bilirubin di-glucuronide when primary hepatocytes were used, whereas it was not observed in HepG2 under the same 3D culture system (Hirano et al. 2020). Therefore, the use of canine and human primary hepatocytes in a 3D culture system may offer a biologically relevant *in vitro* model preserving the function of drug-metabolizing enzymes in the cytoplasm,

mitochondria, and cell membrane transporters. In the present study, the *in vitro* assessment of bilirubin glucuronidation activity using a 3D culture system demonstrated the generation of mono- and di-glucuronic acid conjugates in both canine and human primary hepatocytes, with no comparative measurement of UGT1A1 in 2D and 3D culture systems for primary hepatocytes.

UGT1A1 in the UGT1A subfamily also catalyzes bilirubin glucuronidation in dogs. Species differences in bilirubin glucuronidation activity have been established between humans and dogs, utilizing liver microsomes and recombinant UGT1A1, with dogs exhibiting lower activity than humans (Soars et al. 2001, Troberg et al. 2015). Further insights into species differences can be gained by monitoring enzyme expression kinetics at the mRNA and protein levels, alongside assessing metabolite appearance due to UGT1A1 activity through specific enzyme inhibition using chemicals or siRNA. Nevertheless, species differences in the activity may be partially attributed to amino acid sequence variations affecting bilirubin metabolism, particularly concerning genetic polymorphisms of UGT1A1 in humans (Aono et al. 1995, Kadakol et al. 2000). In the present study, the bilirubin glucuronidation activity in canine and human primary hepatocytes cultured in a 3D culture system using cell-culture plates was examined and compared. Human bilirubin glucuronidation activity was significantly higher than that in dogs on days 7 and 14, consistent with prior reports (Soars et al. 2001, Troberg et al. 2015). It has been reported that human primary hepatocytes maintained a spherical morphology for 21 days on cell culture plates, with albumin secretion, one of the indicators of spheroid activity, by the formation of spheroids increased until day 7 and then decreased at day 14 (Ogihara et al. 2017). Although the albumin secretion was not assessed in this study, no significant difference in bilirubin glucuronidation activity was observed between days 7 and 14.

This 3D culture system assay could offer supplemetary information to bilirubin glucuronide activity in dogs.

In conclusion, this study detected the generation of mono- and di-glucuronic acid conjugates in canine and human primary hepatocytes by assessing bilirubin-glucuronidation activity *in vitro* using a 3D culture system. Furthermore, species differences in bilirubin glucuronidation activity have been identified between humans and dogs, with human activity surpassing that of dogs. The findings suggests that primary hepatocytes cultured in a 3D culture system can serve as a valuable *in vitro* system for the comprehensive evaluation of bilirubin glucuronidation in both humans and dogs, and can be developed into a detailed study to analyze the mechanism of species differences. Therefore, we aim to develop a three-dimensional culture system for evaluation using primary hepatocytes from other animal species in the future.

3. EVALUATING VARIATIONS IN BILIRUBIN GLUCURONIDATION ACTIVITY BY PROTEASE INHIBITORS IN CANINE AND HUMAN PRIMARY HEPATOCYTES CULTURED IN A 3D CULTURE SYSTEM

3.1. Introduction

Bilirubin, resulting from heme catabolism, is a toxic substance. In the bloodstream, unconjugated bilirubin bound to albumin is transported to the liver through organic anion-transporting polypeptide (OATP) 1B1 and OATP1B3 (Cui et al., 2001). Subsequently, bilirubin binds to ligandin and is transported to the endoplasmic reticulum, where it undergoes conjugation with glucuronic acid in the cytoplasm of hepatocytes (Chang et al., 2013; Sticova and Jirsa, 2013). UDP-glucuronosyltransferase (UGT) 1A1 primarily catalyzes this conjugation, and conjugated bilirubin is then excreted into bile via multidrug resistance-associated protein 2 (MRP2) (Chang et al., 2013; Jedlitschky et al., 1997). Impaired bilirubin conjugation, either due to the compound-induced inhibition of UGT1A1 or genetic polymorphisms in UGT1A1, has consequences for bilirubin clearance (Aono et al., 1995; Bosma et al., 1995; Erlinger et al., 2014; Roy-Chowdhury et al., 2017). This not only holds clinical significance but also serve as a potential platform for *in vitro* assessment of drug metabolism.

Hepatocytes and liver microsomes are commonly employed *in vitro* to investigate drug metabolism (Brandon et al., 2003). Hepatocytes, which are fully equipped with drug-metabolizing enzymes, demonstrate greater efficiency in generating biologically relevant metabolite profiles compared to liver microsomes (Dalvie et al., 2009). However, drug metabolism activities in hepatocytes under conventional two-dimensional (2D) conditions differ from those under *in vivo* conditions due to phenotypic changes, such as altered expression of drug-metabolizing enzymes or morphological shifts (Hewitt et al., 2007; Ohkura et al., 2014). To overcome these limitations associated with 2D hepatocyte cultures, three-dimensional (3D)

culture systems have been recently developed. These systems, utilizing spheroids formed by hepatocyte aggregation, replicate a natural physiological environment, enabling the maintenance of mature hepatic phenotypes and stable hepatic functionality over the long term (Lauschke et al., 2019). The 3D culture systems find applications in drug metabolism studies involving liver cell lines like HepG2, HepaRG, and primary hepatocytes (Bell et al., 2016; Ohkura et al., 2014; Ramaiahgari et al., 2014; Takahashi et al., 2015). Notably, the evaluation of bilirubin glucuronidation activity in HepG2 cells cultured under 2D conditions and a 3D culture system using cell-able plates demonstrated the usefulness of the 3D culture system in assessing bilirubin metabolic properties (Hirano et al., 2020).

In the development of medicinal drugs, pre-clinical toxicity studies involving rodents and non-rodents, such as rats and canines, are imperative for safety assessments. However, variations in toxicity test results may arise among animal species. For instance, the bilirubin glucuronidation activity differs between humans and canines, with canines exhibiting lower activity that in humans, as observed using liver microsomes and recombinant UGT1A1 (Soars et al., 2001; Troberg et al., 2015). Nonetheless, there is limited information regarding the *in vitro* evaluation of liver cell lines or primary hepatocytes.

In the present study, primary canine and human hepatocyte spheroids were subjected to atazanavir, indinavir, ritonavir, and nelfinavir, associated with hyperbilirubinemia *in vitro* (Chang et al., 2013). The variations in bilirubin metabolic function in both hepatocyte spheroids were compared by examining the formation of bilirubin glucuronides.

3.2. Materials and methods

3.2.1. Cell culture

Bilirubin, acetonitrile, telmisartan, ammonium acetate, and dimethyl sulfoxide (DMSO) were purchased from FUJIFILM Wako Pure Chemical Corporation (Osaka, Japan). Culture media were purchased from Thermo Fisher Scientific (Waltham, MA, USA), unless otherwise stated. Cryopreserved primary hepatocytes from beagle dogs (male, 5-month-old) and humans (five donors, two lots of hepatocytes aged 22–74 years old and 50–64 years old) were obtained from Thermo Fisher Scientific.

Canine and human primary hepatocytes were cultured for up to 15 days, according to the method of Ikeda et al. (2012), with minor modifications, which involved a microfabricated cell array system. Briefly, canine and human primary hepatocytes were thawed and prepared in William's medium E supplemented with a hepatocyte plating supplement pack (CM3000) and cryopreserved hepatocyte recovery medium (CM7000), respectively. Cells were seeded at a density of 5.0×10^4 cells/well in 96-well 3D culture plates (Cell-able BP-96-R800, Toyo Gosei Co., Ltd., Tokyo, Japan), which have 800 spheroid-forming regions with a diameter of approximately 100 μm in one well, and cultured in William's medium E supplemented with CM3000 at 37°C and 5% CO_2. The seeding medium was replaced with 70 μL of William's medium E supplemented with a hepatocyte maintenance supplement pack (CM4000) one day after seeding. The maintenance medium was replaced with 60 μL fresh medium every 2–3 days.

3.2.2. Albumin enzyme-linked immunosorbent assay

The concentrations of canine and human albumin in culture supernatant collected on days 3, 8, 11, and 15 were measured according to the manufacturer's protocol using an albumin

enzyme-linked immunosorbent assay (ELISA) Kit (Canine: ab157695, Human: ab108788) purchased from Abcam plc (Cambridge, UK). The collected culture supernatants were stored at -80℃ until assay, and diluted 50–300 folds for the assay. The absorbance (450 nm) was measured using a Cytation 5 cell imaging multimode reader (BioTek Instruments, VT, USA).

3.2.3. Quantitative polymerase chain reaction

Total RNA was extracted from canine and human primary hepatocytes cultured in a 3D culture system using the RNeasy® Plus Micro Kit (QIAGEN N.V., Hilden, Germany). Reverse transcription was performed to obtain cDNA using the SuperScript™ IV VILO™ Master Mix (Thermo Fisher Scientific). cDNA was amplified on an ABI 7500 real-time PCR system using TaqPath™ qPCR Master Mix, CG (Thermo Fisher Scientific). The thermal cycling program used was as follows: UNG incubation, 50℃ for 2 min; initial denaturation, 95℃ for 10 min; polymerase chain reaction (40 cycles), 95℃ for 15 s (denaturation) and 55℃ for 1 min (annealing/extension). Glyceraldehyde 3-phosphate dehydrogenase (GAPDH) was used as an internal control. The relative expression of *UGT1A1* was determined using the ΔΔCT method (Livak and Schmittgen, 2001). The sequences of all the primers are listed in Supplementary Table 1.

Supplementaly Table 1: Canine and human common probe and primer sequences for quantitative real-time polymerase chain reaction

Gene	Probe	Forward	Reverse
GAPDH	5′-FAM CCATCTTCCAGGAGCGAGATCC TAMRA-3′	ACCAGGGCTGCTTTTAACTC	TTCTCCATGGTGGTGAAGAC
UGT1A1	5′-FAM ATTGCTGATGCTTTGGGCAAAAT TAMRA-3′	ATGCTTCTGGAGAACATGGA	GCATTGTCCATCTGATCACC

3.2.4. Cell treatment

Canine and human primary hepatocytes cultured in the 3D culture system were treated with atazanavir (FUJIFILM Wako Pure Chemical Corporation), indinavir (MedChemExpress,

NJ, USA), ritonavir (FUJIFILM Wako Pure Chemical Corporation), and nelfinavir (Tokyo Chemical Industry Co., Ltd., Tokyo, Japan) at concentrations of 0, 1, 3.16, 10, 31.6, and 100 µM in a humidified incubator at 37°C and 5% CO_2, after 6 days of seeding (Figure 7). The concentration range was selected to confirm the functional change based on the hepatotoxicity evaluation in primary hepatocyte spheroids cultured in a cell-able plate (Ogihara et al., 2017). DMSO was used as the vehicle for each compound and was added in the reaction corresponding to 0 µM. Since the protease inhibitors have been reported to inhibit not only UGT1A1 that catalyzes bilirubin glucuronidation, but also OATP1B1 and OATP1B3 that facilitate uptake of bilirubin into the hepatocytes (Chang et al., 2013), the primary hepatocytes were treated with the test compounds before bilirubin addition. Approximately 24 h after treatment with each compound, 10 µM bilirubin was added simultaneously in each reaction and incubated for 24 h under the same culture conditions. Further, for bilirubin glucuronidation assessment, 50 µL of the culture supernatant was collected and mixed with an equal amount of ice-cold 100% acetonitrile, to terminate the reaction. Subsequently, the samples were centrifuged at 11,100 × *g* for 15 min at 4°C, and the supernatants were stored at -80°C until analysis.

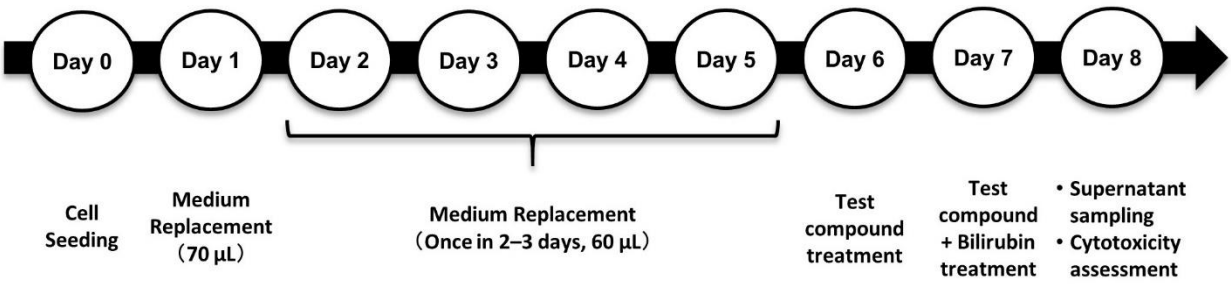

Figure 7: Schematic representation from cell seeding to a test compound and bilirubin treatment, supernatant sampling, and cytotoxicity assessment in the 3D culture.

3.2.5. Cell viability assay

Cells in the wells from which the culture supernatant was collected were used to evaluate viability. The viability of cultured canine and human primary hepatocytes was examined using the Cell Titer-Glo® 3D cell viability assay kit (Promega, Madison, WI, USA) after incubation with the compound and bilirubin on day 8. Briefly, a volume of Cell Titer-Glo® 3D reagent equal to the volume of the cell culture medium in each well (50 µL) was added to the wells. The contents of the wells were vigorously mixed for 30 min, to induce cell lysis. This mixture was diluted four-fold and the luminescent signal was measured using a Cytation 5 cell imaging multimode reader (BioTek Instruments) as an indicator of cell viability.

3.2.6. Liquid chromatography–mass spectrometry

Liquid chromatography–mass spectrometry (LC-MS) analysis was performed as previously described by Omori et al. (2022). The internal standard (IS) stock solution was prepared by dissolving telmisartan in DMSO to a final concentration of 100 µg/mL. The working IS solution (100 ng/mL) was prepared by diluting the stock solution with acetonitrile. A total of 20 µL of the sample, 10 µL of IS working solution, and 60 µL of 10 mM ammonium acetate/acetonitrile (50:50, v/v) were mixed and centrifuged at 2,000 × *g* for 2 min at 5°C. After centrifugation, aliquots (10 µL) of culture supernatants were injected into the LC-MS system. The quantification of bilirubin, bilirubin mono-glucuronide, and bilirubin di-glucuronide was performed using high-performance liquid chromatography (HPLC; Shimadzu Prominence UFLC, Shimadzu Corporation, Kyoto, Japan) coupled with an electrospray ionization mass spectrometer (AB SCIEX Triple Quad 4500). HPLC separation was performed using an Accucore C18 column (2.6 µm, 2.1 × 50 mm, Thermo Fisher Scientific). The mass spectrometer was operated in the positive ion mode. Mass spectrometry data were collected through single-ion monitoring as $[M+H]^+$ ions at 585 m/z for bilirubin, 761 m/z for bilirubin mono-glucuronide, 937

m/z for bilirubin di-glucuronide, and 515 m/z for telmisartan. System operation and data processing for LC-MS were performed using the Analyst 1.6.3 software (AB Sciex Pte. Ltd., Tokyo, Japan). The relative amounts of bilirubin mono-glucuronide and di-glucuronide in canine and human primary hepatocytes were expressed as the target area divided by the IS area in the LC-MS system. The generation of bilirubin glucuronides was expressed as the relative amount divided by the luminescence value of the Cell Titer-Glo® 3D cell viability assay, which is an index of viability. This value was calculated using the following equation:

$$\text{Generation of bilirubin glucuronides} = \frac{\text{Relative amounts of bilirubin glucuronides}^{w}}{\text{Luminescence value of 3D cell viability assay}}$$

In this equation, *w* is the value of the target area which was divided by the IS area for each bilirubin glucuronide in the LC-MS system.

3.2.7. Statistical analyses

The relative expression of *UGT1A1* in canine and human primary hepatocytes cultured for 8 days was initially examined for homogeneity of variances using the F test, and the variances were considered to be equal at $p \geq 0.05$ and unequal at $p < 0.05$. Further, the data were examined using Student's t-test (the variances were equal: parametric), where the level of significance was set at $p < 0.05$, < 0.01, or < 0.001. The generation of bilirubin glucuronides treated with each compound in canines and humans was initially examined for homogeneity of variances using Bartlett's test, and the variances were considered equal at $p \geq 0.01$ and unequal at $p < 0.01$. Then, the data were examined using a Williams-type multiple comparison test (if the variances were equal: parametric) or Shirley–Williams-type multiple comparison test (if the variances were unequal: nonparametric). For each multiple comparison test, the level of significance was set at $p < 0.025$, < 0.005, or < 0.0005.

3.3. Results

When canine and human primary hepatocytes were cultured for spheroid development using the cell array system for up to 15 days, albumin levels peaked on days 3 to 8 in canine hepatocyte spheroids and on day 8 in human hepatocyte spheroids, and subsequently decreased toward day 15 in both spheroids (Figure 8a, b). Spheroids with distinct shapes were formed in both canine and human hepatocytes on day 8 (Figure 8c, d). Furthermore, the relative expression of *UGT1A1*, which catalyzed bilirubin glucuronidation in canine and human primary hepatocyte spheroids cultured for 8 days in the 3D culture system was significantly higher ($p<0.001$) in humans than that in canines (Figure 8e).

When canine and human primary hepatocytes were cultured for 6 days and then treated with atazanavir, indinavir, ritonavir, or nelfinavir for 2 days, treatment with atazanavir (100 μM), ritonavir (100 μM), and nelfinavir (≥ 31.6 μM) reduced the viability of both hepatocytes by approximately 50% or more (Figure 9).

Approximately 24 h after treatment with each compound to facilitate the variation in bilirubin metabolic function, 10 μM of bilirubin was simultaneously treated with each compound for 24 h in canine and human primary hepatocytes. Both hepatocyte spheroids were treated with the compound concentration with a survival rate of approximately 50% or more of hepatocytes. In canine primary hepatocytes, treatment with 31.6 μM of atazanavir and ritonavir significantly decreased mono- and di-glucuronide levels ($p<0.0005$), respectively; indinavir treatment (100 μM) also significantly decreased di-glucuronide levels ($p<0.005$) (Figure 10a). Nelfinavir treatment did not decrease glucuronide levels up to 10 μM. In human primary hepatocytes, atazanavir treatment from low doses decreased the levels of these glucuronides, with significant decreases in mono-glucuronide and di-glucuronide levels at doses ≥ 3.16 μM ($p<0.025$) and ≥ 1 μM ($p<0.0005$), respectively (Figure 10b). Ritonavir treatment (≥ 10 μM) significantly decreased

di-glucuronide levels ($p<0.005$). Indinavir treatment resulted in lower mono-glucuronide level at 100 μM and di-glucuronide levels at ≥ 31.6 μM than those in 0 μM, but no statistical differences were found. Nelfinavir did not decrease glucuronide levels up to a concentration of 10 μM.

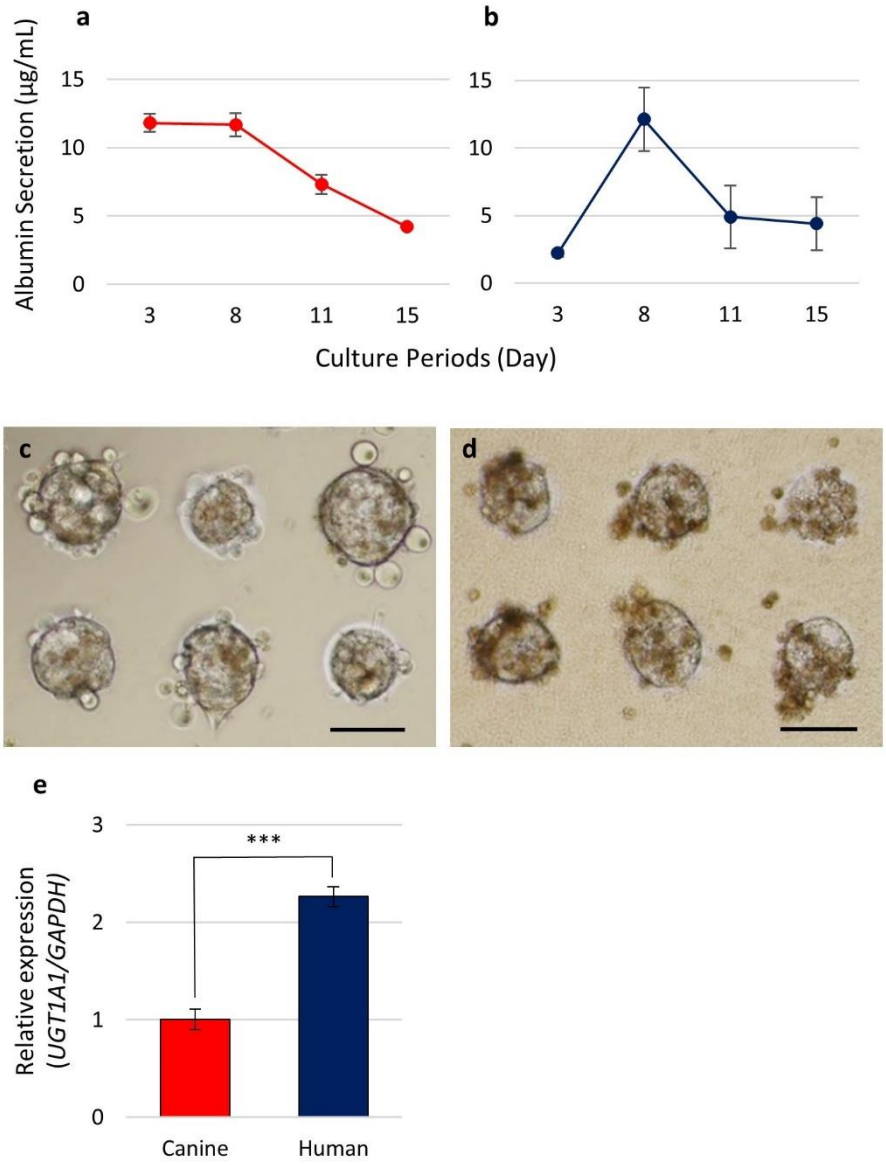

Figure 8: **Albumin secretion from (a) canine and (b) human primary hepatocytes. Each plot indicates the mean ± standard deviation (S.D.) (n = 4). Spheroid development images of (c) canine and (d) human primary hepatocytes on Day 8 in the 3D culture system. Scale bar; 100 µm. (e) Relative expression of *UGT1A1* in canine and human primary hepatocytes on Day 8 in the 3D culture system. Each graph indicates the mean ± S.D. (n = 4). ***: p< 0.001 compared with canines.**

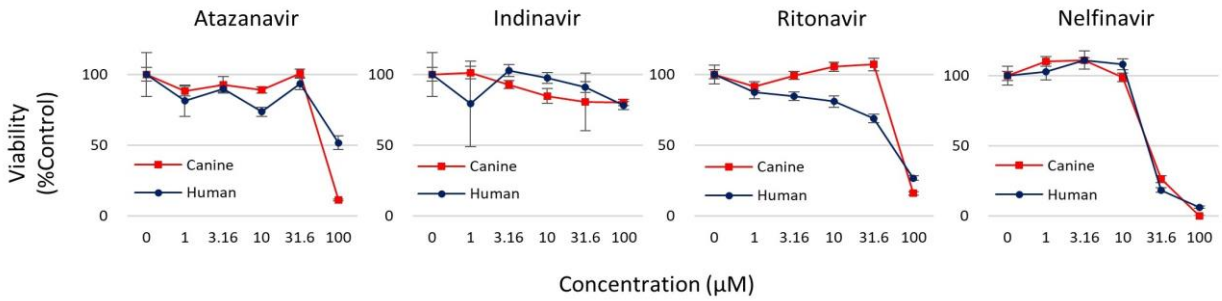

Figure 9: **Viabilities of canine and human primary hepatocytes exposed to atazanavir, indinavir, ritonavir, and nelfinavir for 48 hours. Each graph indicates the mean value (n = 5).**

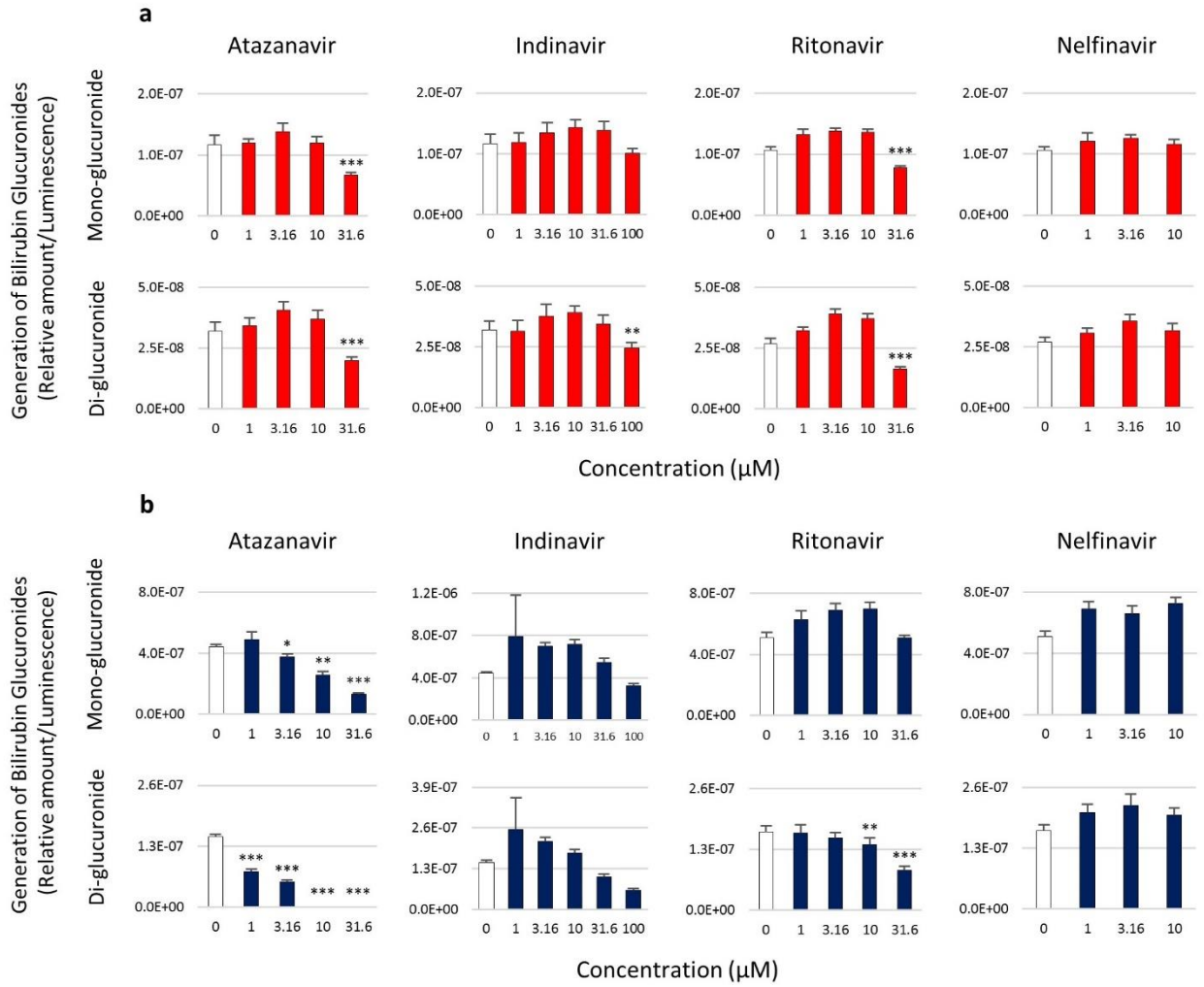

Figure 10: Evaluating the inhibition of bilirubin mono- and di-glucuronide generations after treatment with atazanavir, indinavir, ritonavir, and nelfinavir in (a) canine and (b) human primary hepatocytes cultured in the 3D culture system. Each graph indicates the mean ± S.D. (n = 4–5). *: p< 0.025 **: p< 0.005 ***: p< 0.0005 compared with the 0 μM group.

3.4. Discussion

We recently conducted an assessment of a 3D culture system employing cell-able plates to investigate bilirubin glucuronidation activity in both canine and human hepatocytes (Omori et al., 2022). Our findings confirm the sustained morphology of human hepatocyte spheroids until day 14, consistent with prior reported (Ogihara et al., 2017). Notably, canine hepatocyte spheroids exhibited distinct spheroidal shapes that endured until day 14. In our earlier study, an increase in unintegrated single cells was observed in human hepatocyte spheroids on day 14, indicative of cell death. Additionally, albumin secretion, serving as an indicator of hepatocyte function, peaked around day 8 and declined by day 15 in both canine and human spheroids (Figure 8a, b). These results align with the observations of Ogihara et al. (2017), who reported increased albumin secretion by human hepatocyte spheroids cultured on a cell-able plate until day 7, followed by a decrease on day 14. Significantly, this study marks the first instance of observing albumin secretion by canine hepatocyte spheroids in a 3D culture system. Furthermore, the hepatocyte spheroids on day 8 displayed some blebs but maintained distinct shapes in both canines and humans (Figure 8c, d) and exhibited a similar amount of albumin secretion, indicating that day 8 was deemed optimal for evaluate bilirubin glucuronidation activity.

The culture of the human hepatoma cell line HepG2 in a 3D culture system using a cell-able plate has demonstrated superior efficacy in assessing bilirubin metabolic characteristics compared to a 2D culture system (Hirano et al., 2020). Additionaly, 3D-cultured hepatoma cell lines exhibit heightened expression of metabolic enzymes, including UGT1A1 and transporters, along with enhanced metabolic activities for exogenous compounds (Kobayashi et al., 2012; Ramaiahgari et al., 2014). Hepatoma cell lines generally exhibit lower metabolic enzyme activities than those in primary hepatocytes (Guo et al., 2011; Westerink and Schoonen, 2007;

Wilkening et al., 2003). While bilirubin di-glucuronide has been detected in primary hepatocytes cultured in a 3D culture system using a cell-able plate, the same is not observed with HepG2 cells cultured in the identical plate (Hirano et al., 2020; Omori et al., 2022). Consequently, a comparative analysis of bilirubin glucuronidation activity between 2D and 3D primary hepatocyte cultures may be worthwhile. The utilization of canine and human primary hepatocytes in a 3D culture system appears to represent a biologically relevant *in vitro* model, preserving the functionality of drug-metabolizing enzymes located in the cytoplasm, mitochondria, and cell membrane transporters.

In the present study, the treatment with atazanavir (100 µM), ritonavir (100 µM), and nelfinavir (≥ 31.6 µM) led to a reduction in survival rates to approximately 50% or less in both canine and human primary hepatocyte spheroids (Figure 9). This unequivocally indicates the induction of cell death at these concentrations. Consequently, these concentrations were deemed unsuitable for functional evaluation and were excluded, given the difficulty in determining whether changes in bilirubin glucuronidation activity are attributed to the inhibition of bilirubin metabolism or cell death. Hence, changes in the bilirubin-glucuronide conjugation activity of each drug were analyzed after accounting for cell viability. In a previous study, Chang et al. (2013) evaluated the *in vitro* inhibition of UGT1A1, OATP1B1, OATP1B3, and MRP2 using human liver microsomes, HEK293 cells, and membrane vesicles expressing bile salt export pump (BSEP) and MRP2. They reported relatively high inhibitory activities of atazanavir and ritonavir against UGT1A1, OATP1B1 or OATP1B3. Moreover, atazanavir, indinavir, and ritonavir had similar inhibitory activities against BSEP, but IC_{50} was not calculated for atazanavir, indinavir, ritonavir, or nelfinavir up to 100 µM for MRP2 inhibition. Similarly, in the present study, a substantial inhibition of bilirubin glucuronide formation in the culture

supernatant was observed with atazanavir and ritonavir in human hepatocyte spheroids (Figure 10b). This may reflect their effects on cellular uptake of bilirubin via OATP1B1 or OATP1B3 and its intracellular metabolic function catalyzed by UGT1A1. Canine hepatocyte spheroids exhibited a parallel trend to that observed in humans (Figure 10a). Our findings underscore the potencial utility of primary hepatocytes in a 3D culture system for assessing variations in bilirubin metabolic function.

In this study, we observed that the changes in bilirubin glucuronidation activity induced by each compound were more pronounced in humans than that in canines, with atazanavir showing particularly remarkable effects. Although UGT1A1 catalyzes bilirubin glucuronidation in canines as well (Troberg et al., 2015), *UGT1A1* expression was higher in human hepatocyte spheroids than that in canine hepatocyte spheroids on day 8 (Figure 8e). This suggests that humans may exhibit greater sensitivity to atazanavir, known for its potent UGT1A1 inhibition. Moreover, bilirubin glucuronidation activity using liver microsomes and recombinant UGT1A1 has been reported to be higher in humans than that in canines (Soars et al., 2001; Troberg et al., 2015). Chang et al. (2013) reported a lower IC_{50} for UGT1A1 inhibition for atazanavir (0.31 μM) compared to ritonavir (3.1 μM), nelfinavir (4.8 μM), and indinavir (6.8 μM). The substantial difference between atazanavir and ritonavir in their study, approximately 10-fold, may explain why the species difference in atazanavir effects on bilirubin glucuronidation activity was more significant. Additionally, species differences in activity may be attributed, in part, to variations in amino acid sequences concerning the impact of bilirubin metabolism on genetic polymorphisms of *UGT1A1* in humans (Aono et al., 1995; Kadakol et al., 2000).

In conclusion, we have identified suitable conditions for evaluating the variations in bilirubin metabolic function in primary canine and human hepatocyte spheroids using small-

molecule drugs. This approach allows for a comprehensive assessment of bilirubin metabolic function, considering physiological conditions such as intracellular and extracellular transport, metabolic enzyme reactions, and cytotoxicity. The findings suggest that primary hepatocytes cultured in a 3D culture system may serve as a valuable *in vitro* system for the risk assessment in bilirubin metabolic disorders during drug development.

4. OVERALL DISCUSSION

To date, reports on human hepatocyte culture in a 3D system have been published (Ogihara et al. 2017, Ohkura et al. 2014); however, but there is a lack of information on *in vitro* evaluation using canine primary hepatocytes in such a 3D system. In this study, canine and human primary hepatocytes cultured for 7 and 14 days on 3D culture plates (Cell-able plates) formed distinct spherical structures and maintained their morphology until day 14 (Figure 4). A comparative analysis of canine and human hepatocyte spheroids on days 7 and 14 revealed a more distinct spherical shape in canine spheroids. In contrast, human spheroids showed an increase in single cells on day 14 (Figure 4d), indicating their potential to induce cell death. Moreover, albumin secretion, which reflects hepatocyte function, reached its highest level around day 8 and declined by day 15 in both canine and human spheroids (Figure 8a, b). These observations are consistent with a previous study by Ogihara et al. (2017), who reported a similar pattern of increased albumin secretion in human hepatocyte spheroids until day 7, followed by a decrease on day 14.

This study further highlights the effectiveness of the 3D culture system for assessing bilirubin metabolic characteristics in human hepatocytes compared with the human hepatoma cell line HepG2 in a 2D system. Bilirubin di-glucuronide was detected when a primary hepatocyte was used in this study (Figure 6); however, it was not detected in HepG2 cells grown in the same 3D culture system (Hirano et al., 2020). Additionally, this study explored species differences in bilirubin glucuronidation activity between humans and dogs, noting a higher activity in humans (Figure 6), consistent with previous reports (Soars et al. 2001, Troberg et al. 2015).

Protease inhibitors, such as atazanavir, indinavir, ritonavir, and nelfinavir, on canine and human primary hepatocyte spheroids evaluated their effects on bilirubin glucuronidation activity, revealing a substantial reduction in survival rates at specific concentrations, indicating cell death (Figure 9). Consequently, concentrations that reduced viability by approximately 50% or more were deemed unsuitable for functional evaluation because it may be difficult to determine whether the change in bilirubin glucuronidation activity was due to the inhibition of bilirubin metabolism or cell death.

Chang et al. (2013) investigated *in vitro* inhibition of UGT1A1, OATP1B1, OATP1B3, BSEP, and MRP2 in human liver microsomes, HEK293 cells, and membrane vesicles. They reported high inhibitory activities of atazanavir and ritonavir against UGT1A1, OATP1B1, or OATP1B3. Additionally, atazanavir, indinavir, and ritonavir exhibited similar inhibitory activities against BSEP, with no calculated IC_{50} for atazanavir, indinavir, ritonavir, or nelfinavir up to 100 µM for MRP2 inhibition.

This current study observed substantial inhibition of bilirubin glucuronide formation in human hepatocyte spheroids by atazanavir and ritonavir (Figure 10b), indicating the potential effects on bilirubin uptake via OATP1B1 or OATP1B3 and intracellular metabolic functions mediated by UGT1A1. Canine hepatocyte spheroids exhibited a trend similar to that observed in human hepatocytes (Figure 10a), suggesting the utility of primary hepatocytes in a 3D culture system for assessing variations in bilirubin metabolic function.

This study observed more pronounced changes in bilirubin glucuronidation activity caused by each compound in humans than in canines, particularly for atazanavir. While both species expressed UGT1A1, which catalyzes bilirubin glucuronidation (Troberg et al., 2015), human hepatocyte spheroids exhibited higher *UGT1A1* expression on day 8 than canine hepatocyte

spheroids (Figure 8e). This suggests that humans are more sensitive to atazanavir, which potently inhibits UGT1A1. Additionally, human bilirubin glucuronidation activity in liver microsomes and recombinant UGT1A1 is higher than that in canines (Soars et al., 2001; Troberg et al., 2015). Chang et al. (2013) reported lower IC_{50} values for UGT1A1 inhibition in the order of atazanavir (0.31 μM), ritonavir (3.1 μM), nelfinavir (4.8 μM), and indinavir (6.8 μM), with atazanavir being more potent than others. It found a 10-fold difference between atazanavir and ritonavir, potentially explaining why species differences in atazanavir had a more pronounced effects on bilirubin glucuronidation activity.

In conclusion, this study utilized a 3D culture system to detect the generations of mono- and di-glucuronic acid conjugates in canine and human primary hepatocytes by assessing bilirubin-glucuronidation activity *in vitro*. This investigation revealed species differences in bilirubin glucuronidation activity, with humans exhibiting higher activity than dogs. Additionally, this study confirmed the suitable conditions for assessing the variation in bilirubin metabolic function using small-molecule drugs, emphasizing the utility of 3D culture system for the risk assessment of bilirubin metabolic disorders during drug development. These findings suggest that the 3D culture system with primary hepatocytes could serve as a valuable *in vitro* tool for the comprehensive evaluation of bilirubin glucuronidation in both species, prompting further detailed studies to analyze the underlying mechanisms of these species differences.

5. OVERALL SUMMARY

Species differences in bilirubin glucuronidation activity are observed between humans and dogs through liver microsomes and recombinant UDP-glucuronosyltransferase 1A1. Humans exhibit higher activity than that of dogs. In this study (Heading 1: Omori et al., 2022), bilirubin glucuronidation activity was examined in canine and human primary hepatocyte spheroids formed using a 3D culture system. When spheroid development in canine and human primary hepatocytes was evaluated on days 7 and 14 after the start of culture, canine primary hepatocyte spheroids had a more distinct spherical shape than human hepatocyte spheroids, irrespective of the culture period. Furthermore, mono- and di-glucuronide generation detected in spheroids were significantly higher ($P < 0.05$) in human primary hepatocytes than in canine primary hepatocytes after 24 hours of incubation with bilirubin for each culture period. These results suggest that there are species differences in the bilirubin glucuronidation activity of primary hepatocytes with spheroid formation between humans and dogs, with the activity being higher in humans than in dogs.

Bilirubin is excreted into the bile from hepatocytes, mainly as monoglucuronosyl and bisglucuronosyl conjugates, reflecting bilirubin glucuronidation activity. However, there is limited information on the *in vitro* evaluation of liver cell lines or primary hepatocytes. This study (Heading 3: Omori et al., 2023) aimed to investigate variations in the bilirubin metabolic function of canine and human hepatocyte spheroids formed in a three-dimensional (3D) culture system indicated by the formation of bilirubin glucuronides when protease inhibitors such as atazanavir, indinavir, ritonavir, and nelfinavir were treated with bilirubin. The culture supernatant was collected for bilirubin glucuronidation assessment, and the cells were used to

evaluate viability. On day 8 of culture, both canine and human hepatocyte spheroids showed high albumin secretion and distinct spheroid formation, and their bilirubin glucuronidation activities were evaluated considering cell viability. Treatment with atazanavir and ritonavir remarkably inhibited bilirubin glucuronide formation, wherein atazanavir showed the highest inhibition, particularly in human hepatocyte spheroids. These results may reflect the effects on cellular uptake of bilirubin and its intracellular metabolic function. Thus, primary hepatocytes cultured in a 3D culture system may be a useful *in vitro* system for the comprehensive evaluation of bilirubin metabolic function and risk assessment in bilirubin metabolic disorders for drug development.

6. ACKNOWLEGEMENT

I most sincerely appreciate the constant support and encouragement of my supervisor, Prof. Dr. Takeshige Otoi. His guidance helped me in conducting this study and writing the dissertation.

My heartiest thanks to the rest of my thesis committee: Prof. Dr. Taro Mito and Prof. Dr. Yoshihiro Uto, for their insightful comments and encouragement. I would also like to express my sincere gratitude to Lecturer Dr. Maki Hirata for her support and cooperation. Without them, this research would not have been well guided. Thank you to my laboratory colleagues for their cooperation, kind help, and good times over the past three years.

7. REFERENCES

Aono, S., Adachi, Y., Uyama, E., Yamada, Y., Keino, H., Nanno, T., Koiwai, O., Sato, H., 1995. Analysis of genes for bilirubin UDP-glucuronosyltransferase in Gilbert's syndrome. Lancet. 345:958-959. https://doi.org/10.1016/s0140-6736(95)90702-5.

Bell, CC., Hendriks, DF., Moro, S.M., Ellis, E., Walsh, J., Renblom, A., Fredriksson, Puigvert, L., Dankers, AC., Jacobs, F., Snoeys, J., Sison-Young, R.L., Jenkins, R.E., Nordling, A., Mkrtchian, S., Park, B.K., Kitteringham, N.R., Goldring, C.E., Lauschke, V.M., Ingelman-Sundberg, M., 2016. Characterization of primary human hepatocyte spheroids as a model system for drug-induced liver injury, liver function and disease. Sci. Rep. 6, 25187. https://doi.org/10.1038/srep25187.

Bosma, PJ., Chowdhury, JR., Bakker, C., Gantla, S., de Boer, A., Oostra, B.A., Lindhout, D., Tytgat, G.N., Jansen, P.L., Oude, Elferink, RP., Chowdhury, N.R., 1995. The genetic basis of the reduced expression of bilirubin UDP-glucuronosyltransferase 1 in Gilbert's syndrome. N. Engl. J. Med. 333, 1171-1175. https://doi.org/10.1056/NEJM199511023331802.

Brandon, E.F.A., Raap, C.D., Meijerman, I., Beijnen, J.H., Schellens, J.H.M., 2003. An update on *in vitro* test methods in human hepatic drug biotransformation research: pros and cons. Toxicol. Appl. Pharmacol. 189, 233-246. https://doi.org/10.1016/S0041-008X(03)00128-5.

Chang, J.H., Plise, E., Cheong, J., Ho, Q., Lin, M., 2013. Evaluating the *in vitro* inhibition of UGT1A1, OATP1B1, OATP1B3, MRP2, and BSEP in predicting drug-induced hyperbilirubinemia. Mol. Pharm. 10, 3067-3075. https://doi.org/10.1021/mp4001348.

Chen, S., Tukey, RH., 2018. Humanized UGT1 Mice, Regulation of UGT1A1, and the Role of the Intestinal Tract in Neonatal Hyperbilirubinemia and Breast Milk-Induced Jaundice. Drug Metab Dispos. 46, 1745-1755. https://dmd.aspetjournals.org/content/46/11/1745

Cui, Y., König, J., Leier, I., Buchholz, U., Keppler, D., 2001. Hepatic uptake of bilirubin and its conjugates by the human organic anion transporter SLC21A6. J. Biol. Chem. 276, 9626–9630. https://doi.org/10.1074/jbc.M004968200.

Dalvie, D., Obach, R.S., Kang, P., Prakash, C., Loi, CM., Hurst, S., Nedderman, A., Goulet, L., Smith, E., Bu, H.Z., Smith, D.A., 2009. Assessment of three human *in vitro* systems in

the generation of major human excretory and circulating metabolites. Chem. Res. Toxicol. 22, 357-368. https://doi.org/10.1021/tx8004357.

Erlinger, S., Arias, I.M., Dhumeaux, D., 2014. Inherited disorders of bilirubin transport and conjugation: new insights into molecular mechanisms and consequences. Gastroenterology. 146, 1625-1638. https://doi.org/10.1053/j.gastro.2014.03.047.

Guo, L., Dial, S., Shi, L., Branham, W., Liu, J., Fang, J.L., Green, B., Deng, H., Kaput, J., Ning, B. 2011. Similarities and differences in the expression of drug-metabolizing enzymes between human hepatic cell lines and primary human hepatocytes. Drug Metab. Dispos. 39, 528-538. https://doi.org/10.1124/dmd.110.035873.

Hewitt, NJ., Lechón, MJ., Houston, J.B., Hallifax, D., Brown, H.S., Maurel, P., Kenna, J.G., Gustavsson, L., Lohmann, C., Skonberg, C., Guillouzo, A., Tuschl, G., Li, A.P., LeCluyse, E., Groothuis, G.M., Hengstler, J.G., 2007. Primary hepatocytes: current understanding of the regulation of metabolic enzymes and transporter proteins, and pharmaceutical practice for the use of hepatocytes in metabolism, enzyme induction, transporter, clearance, and hepatotoxicity studies. Drug Metab. Rev. 39, 159-234. https://doi.org/10.1080/03602530601093489.

Hirano, T., Hirata, M., Fujimoto, S., Nguyen, N.T., Le, Q.A., Tanihara, F., Otoi, T., 2020. Comparative analysis of bilirubin glucuronidation activity in 2D- and 3D-cultured human hepatocellular carcinoma HepG2 cells. In Vitro Cell. Dev. Biol. Anim. 56, 277–280. https://doi.org/10.1007/s11626-020-00451-8.

Ikeda, Y., Jomura, T., Horiuchi, U., Saeki, J., Yoshimoto, K., Ikeya, T., Nagasaki, Y., 2012. Long-term survival and functional maintenance of hepatocytes by using a microfabricated cell array. Colloids Surf. B Biointerfaces. 97, 97–100. https://doi.org/10.1016/j.colsurfb.2012.04.022.

Jedlitschky, G., Leier, I., Buchholz, U., Hummel-Eisenbeiss, J., Burchell, B., Keppler, D., 1997. ATP-dependent transport of bilirubin glucuronides by the multidrug resistance protein MRP1 and its hepatocyte canalicular isoform MRP2. Biochem. J. 327, 305–310. https://doi.org/10.1042/bj3270305.

Kadakol, A., Ghosh, S.S., Sappal, B.S., Sharma, G., Chowdhury, J.R., Chowdhury, N.R., 2000. Genetic lesions of bilirubin uridine-diphosphoglucuronate glucuronosyltransferase (UGT1A1) causing Crigler-Najjar and Gilbert syndromes: correlation of genotype to

phenotype. Hum. Mutat. 16, 297-306. https://doi.org/10.1002/1098-1004(200010)16:4<297::AID-HUMU2>3.0.CO;2-Z.

Kobayashi, K., Yoshida, A., Ejiri, Y., Takagi, S., Mimura, H., Hosoda, M., Matsuura, T., Chiba, K., 2012. Increased expression of drug-metabolizing enzymes in human hepatocarcinoma FLC-4 cells cultured on micro-space cell culture plates. Drug Metab. Pharmacokinet. 27, 478-485. https://doi.org/10.2133/dmpk.dmpk-12-rg-016.

Lauschke, V.M., Shafagh, R.Z., Hendriks, D.F.G., Ingelman-Sundberg, M., 2019. 3D primary hepatocyte culture systems for analyses of liver diseases, drug metabolism, and toxicity: emerging culture paradigms and applications. Biotechnol. J. 14, e1800347. https://doi.org/10.1002/biot.201800347.

Livak, K.J., Schmittgen, T.D., 2001. Analysis of relative gene expression data using real-time quantitative PCR and the $2^{-\Delta\Delta CT}$ method. Methods. 25, 402–408. https://doi.org/10.1006/meth.2001.1262.

Ma, G., Lin, J., Cai, W., Tan, B., Xiang, X., Zhang, Y., Zhang, P., 2014. Simultaneous determination of bilirubin and its glucuronides in liver microsomes and recombinant UGT1A1 enzyme incubation systems by HPLC method and its application to bilirubin glucuronidation studies. J Pharma Biomed Anal 92, 149-159. https://doi.org/10.1016/j.jpba.2014.01.025.

Ogihara, T., Arakawa, H., Jomura, T., Idota, Y., Koyama, S., Yano, K., Kojima, H., 2017. Utility of human hepatocyte spheroids without feeder cells for evaluation of hepatotoxicity. J. Toxicol. Sci. 42, 499–507. https://doi.org/10.2131/jts.42.499.

Ohkura, T., Ohta, K., Nagao, T., Kusumoto, K., Koeda, A., Ueda, T., Jomura, T., Ikeya, T., Ozeki, E., Wada, K., Naitoh, K., Inoue, Y., Takahashi, N., Iwai, H., Arakawa, H., Ogihara, T., 2014. Evaluation of human hepatocytes cultured by three-dimensional spheroid systems for drug metabolism. Drug Metab. Pharmacokinet. 29, 373-378. https://doi.org/10.2133/dmpk.dmpk-13-rg-105.

Omori, H., Chikamoto, J., Hirano, T., Besshi, K., Yoshimura, N., Hirata, M., Otoi, T., 2022. Comparative analysis of bilirubin glucuronidation activity in canine and human primary hepatocytes using a 3D culture system. In Vitro Cell. Dev. Biol. Anim. 58, 712-718. https://doi.org/10.1007/s11626-022-00711-9.

Omori, H., Chikamoto, J., Nagahara, M., Hirata, M., Otoi, T., 2023. Evaluating variations in bilirubin glucuronidation activity by protease inhibitors in canine and human primary hepatocytes cultured in a 3D culture system. Toxicol. in vitro. 93. https://doi.org/10.1016/j.tiv.2023.105689.

Ramaiahgari, S.C., den Braver, M.W., Herpers, B., Terpstra, V., Commandeur, J.N., van de Water, B., Price, L.S., 2014. A 3D *in vitro* model of differentiated HepG2 cell spheroids with improved liver-like properties for repeated dose high-throughput toxicity studies. Arch. Toxicol. 88, 1083-1095. https://doi.org/10.1007/s00204-014-1215-9.

Roy-Chowdhury, J., Roy-Chowdhury, N., Listowsky, I., Wolkoff, A.W., 2017. Drug- and drug abuse-associated hyperbilirubinemia: experience with atazanavir. Clin. Pharmacol. Drug Dev. 6, 140–146. https://doi.org/10.1002/cpdd.314.

Soars, M.G., Riley, R.J., Findlay, K.A., Coffey, M.J., Burchell, B., 2001. Evidence for significant differences in microsomal drug glucuronidation by canine and human liver and kidney. Drug Metab. Dispos. 29, 121-126. https://dmd.aspetjournals.org/content/29/2/121.long.

Sticova, E., Jirsa, M., 2013. New insights in bilirubin metabolism and their clinical implications. World J. Gastroenterol. 19, 6398-6407. https://doi.org/10.3748/wjg.v19.i38.6398.

Takahashi, Y., Hori, Y., Yamamoto, T., Urashima, T., Ohara, Y., Tanaka, H., 2015. 3D spheroid cultures improve the metabolic gene expression profiles of HepaRG cells. Biosci. Rep. 35, e00208. https://doi.org/10.1042/BSR20150034.

Troberg, J., Järvinen, E., Muniz, M., Sneitz, N., Mosorin, J., Hagström, M., Finel, M., 2015. Dog UDP-glucuronosyltransferase enzymes of subfamily 1A: cloning, expression, and activity. Drug Metab. Dispos. 43, 107-118. https://doi.org/10.1124/dmd.114.059303.

Wang, Q., Dai, Z., Wen, B., Ma, S., Zhang, Y., 2015. Estimating the Differences of UGT1A1 Activity in Recombinant UGT1A1 Enzyme, Human Liver Microsomes and Rat Liver Microsome Incubation Systems in Vitro. Bio Pharma Bulletin. 38, 1910-1917. https://doi.org/10.1248/bpb.b15-00513.

Westerink, W.M., Schoonen, W.G., 2007. Phase II enzyme levels in HepG2 cells and cryopreserved primary human hepatocytes and their induction in HepG2 cells. Toxicol. in vitro. 21, 1592-1602. https://doi.org/10.1016/j.tiv.2007.06.017.

Wilkening, S., Stahl, F., Bader, A., 2003. Comparison of primary human hepatocytes and hepatoma cell line Hepg2 with regard to their biotransformation properties. Drug Metab. Dispos. 31, 1035-1042. https://doi.org/10.1124/dmd.31.8.1035.